

Unconventional Superconductivity in Heavy Fermion UTe₂

Dai Aoki^{1,2*}, Ai Nakamura¹, Fuminori Honda¹, DeXin Li¹, Yoshiya Homma¹, Yusei Shimizu¹, Yoshiki J. Sato¹, Georg Knebel², Jean-Pascal Brison², Alexandre Pourret², Daniel Braithwaite², Gerard Lapertot², Qun Niu², Michal Vališka², Hisatomo Harima³, and Jacques Flouquet²

¹IMR, Tohoku University, Oarai, Ibaraki, 311-1313, Japan

²University Grenoble Alpes, CEA, IRIG-PHELIQS, F-38000 Grenoble, France

³Graduate School of Science, Kobe University, Kobe 657-8501, Japan

We grew single crystals of the recently discovered heavy fermion superconductor UTe₂, and measured the resistivity, specific heat and magnetoresistance. Superconductivity (SC) was clearly detected at $T_{sc} = 1.65$ K as sharp drop of the resistivity in a high quality sample of $RRR = 35$. The specific heat shows a large jump at T_{sc} indicating strong coupling. The large Sommerfeld coefficient, $\gamma = 117$ mJK⁻²mol⁻¹ extrapolated in the normal state and the temperature dependence of C/T below T_{sc} are the signature of unconventional SC. The discrepancy in the entropy balance at T_{sc} between SC and normal states points out that hidden features must occur. Surprisingly, a large residual value of the Sommerfeld coefficient seems quite robust ($\gamma_0/\gamma \sim 0.5$). The large upper critical field H_{c2} along the three principal axes favors spin-triplet SC. For $H \parallel b$ -axis, our experiments do not reproduce the huge upturn of H_{c2} reported previously. This discrepancy may reflect that H_{c2} is very sensitive to the sample quality. A new perspective in UTe₂ is the proximity of a Kondo semiconducting phase predicted by the LDA band structure calculations.

Unconventional superconductivity (SC) attracts much attention in the strongly correlated electron systems, in particular, the microscopic coexistence of ferromagnetism and SC^{1,2} discovered in UGe₂,³ URhGe,⁴ and UCoGe.⁵ One of the highlights is the field-reentrant (-reinforced) SC^{6,7} in transverse magnetic field with respect to the ferromagnetic (FM) alignment; when the magnetic field is applied along the hard magnetization axis (b -axis) in URhGe and UCoGe, the Curie temperature T_{Curie} is suppressed. The collapse of T_{Curie} enhances the FM fluctuations which boost SC. In addition Fermi surface (FS) instabilities give an extra source for the enhancement of the upper critical field, H_{c2} .⁸⁻¹⁰ Spin-triplet pairing is clearly realized for the three uranium ferromagnets.

Very recently, SC was discovered in the heavy fermion paramagnet UTe₂,¹¹ with a rather high superconducting transition temperature, $T_{sc} = 1.6$ K. Furthermore, from the large H_{c2} , exceeding the Pauli limit, and the constant Knight shift through T_{sc} , the spin-triplet SC seems to occur. The great interest compared to the previous cases is that the ground state is paramagnetic at the verge of FM order above the appearance of SC. In order to study these results in more detail, we grew single crystals and measured the resistivity, specific heat and magnetoresistance at low temperatures.

UTe₂ crystallizes in the body-centered orthorhombic structure (UTe₂-type) with the space group $Immm$ (#71, D_{2h}^{25}). The lattice parameters are $a = 4.165$ Å, $b = 6.139$ Å, and $c = 13.979$ Å. The c -axis is quite long, but the corresponding Brillouin zone is not very flat because of the body-centered orthorhombic structure. A paramagnetic ground state and heavy electronic states with a large Sommerfeld coefficient $\gamma \sim 120$ – 150 mJK⁻²mol⁻¹ have been reported.^{11,12} The magnetic susceptibility shows Curie-Weiss behavior above 150 K with effective moments close to the $5f^2$ or $5f^3$ free ion value, indicating a $5f$ -localized nature at high temperatures. Note that the Weiss temperatures obtained from fits above 150 K

for a , b , and c -axes are negative, suggesting antiferromagnetic interactions at high temperatures. For $H \parallel b$ -axis, the susceptibility shows a broad maximum with $T_{\chi_{max}} \sim 35$ K. The magnetization curve at 2 K is anisotropic. The easy-axis (a -axis) magnetization reaches $0.5 \mu_B/U$ at 7 T, while the hard-axes (c and b -axes) magnetizations are only 0.15 and 0.09 μ_B/U , respectively at 7 T.^{11,12}

Single crystals of UTe₂ were grown using chemical vapor transport (CVT) method with Iodine as transport agent, in Oarai and in Grenoble, as described in Ref. 11. The self-flux method was also used in Oarai. The starting materials with the ratio, U : Te = 22 : 78 (at%) were put into an alumina crucible in a double sealed (tantalum/quartz) ampoule. The Te-flux was removed by spinning off in a centrifuge. The single crystals obtained from both CVT and flux methods were checked by single crystal X-ray analysis. The lattice parameters and the atomic coordinates are well-defined, in good agreement with the previous results.¹² The resistivity at zero field down to 0.1 K was measured by the four-probe AC method. The specific heat was measured by the relaxation method at temperatures down to 0.4 K in PPMS, and at lower temperatures down to 0.1 K in a dilution refrigerator using a homemade calorimetric cell. The magnetoresistance was measured by the four-probe DC method at low temperatures down to 0.03 K, and at high fields up to 15 T in a top-loading dilution refrigerator. The sample with the current along the a -axis was rotated for the field directions from c to b and from b to a . A homemade dilution refrigerator with a 16 T magnet was also used in Grenoble.

Figure 1 shows the temperature dependence of the resistivity for the current along the a -axis of three different samples. The resistivity for the CVT sample (#O) slightly increases linearly down to 50 K and decreases rapidly with further decreasing temperature, indicating typical heavy fermion behavior. At low temperature below ~ 4 K, the resistivity follows a T^2 dependence, indicating Fermi liquid nature, and becomes

*E-mail: aoki@imr.tohoku.ac.jp

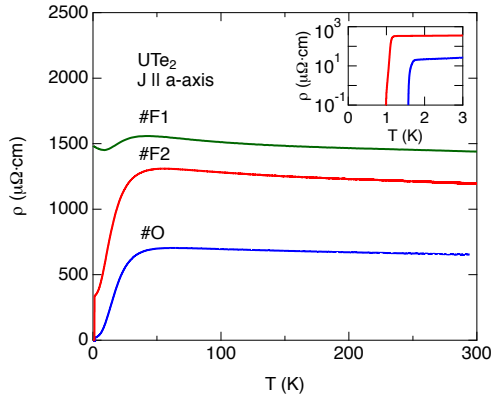


Fig. 1. (Color online) Temperature dependence of the resistivity for the current along a -axis in different samples of UTe_2 . The samples grown using the flux method are denoted by #F1 and #F2. The sample grown using the CVT method is denoted by #O. The inset shows the resistivity at low temperatures for #F2 and #O with the logarithmic scale of vertical axis.

zero, revealing the superconducting transition at $T_{\text{sc}} = 1.65$ K defined by the mid point of the resistivity drop. The residual resistivity ρ_0 and the residual resistivity ratio RRR are $18.5 \mu\Omega \cdot \text{cm}$ and 35, respectively. The A coefficient for the T^2 dependence is $0.88 \mu\Omega \cdot \text{cm}/\text{K}^2$.

Interestingly, the lower quality sample denoted by #F2 (RRR = 4 and $\rho_0 = 340 \mu\Omega \cdot \text{cm}$) also shows the superconducting transition at $T_{\text{sc}} = 1.1$ K. The resistivity at room temperature is nearly twice larger than that for #O. The lowest quality sample (#F1) does not show the superconducting transition down to 0.1 K, instead a small upturn appears.

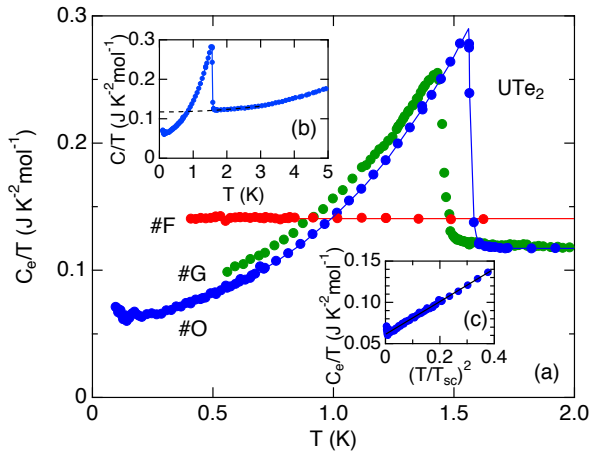


Fig. 2. (Color online) (a) Electronic specific heat in the form of C_e/T vs T for the CVT (#O, #G) and flux (#F) grown samples of UTe_2 . T_{sc} is 1.57 (1.46) K for #O (#G) sample. The small upturn below 0.12 K is most likely due to the nuclear contribution of Te or impurities. (b) The total specific heat in sample #O. The dotted line is the fitting in the normal state to subtract the phonon contribution. (c) The low temperature part of C_e/T in sample #O in the form of C_e/T vs $(T/T_{\text{sc}})^2$.

Figure 2(a) shows the electronic specific heat down to 0.1 K for two CVT (#O, #G) and flux (#F) grown samples. A T^3 phonon contribution is subtracted by fitting the normal state,

as shown in Fig. 2(b). The Sommerfeld coefficient (γ -value) is $\gamma = 117 \text{ mJ K}^{-2} \text{ mol}^{-1}$, indicating the presence of heavy electronic states in UTe_2 . Bulk SC is clearly demonstrated by the large and sharp specific heat jump with $\Delta C_e/\gamma T_{\text{sc}} = 1.51$ and $T_{\text{sc}} = 1.57$ K for #O sample, compared to the weak coupling BCS value ($\Delta C_e/\gamma T_{\text{sc}} = 1.43$). At low temperatures, C_e varies as $\gamma_0 T + \eta T^3$ as shown in Fig. 2(c) for sample #O. These results together with the field dependence of C/T ¹³⁾ are not at all consistent with that for the conventional BCS type.

Remarkably, a large residual γ -value ($\gamma_0 \sim 61 \text{ mJ K}^{-2} \text{ mol}^{-1}$), which is equivalent to $\sim 50\%$ of the normal state γ -value, is observed consistently on all SC samples for $T \rightarrow 0$ K, despite the fact that a sharp specific heat jump is detected at T_{sc} . A large residual γ -value, γ_0 , is observed in FM superconductors, with γ_0 proportional to the square root of the ordered moment, M_0 , ($\gamma_0 \propto M_0^{1/2}$).²⁾ If UTe_2 is a paramagnet down to 0 K, such a large residual γ -value is not expected.

Compared to the previous report,¹¹⁾ both the data in #O and #G samples confirm that the residual term remains always very close to 50% of the normal state γ -value. The explanation for this term¹¹⁾ is that only half the FS would be paired, as it happens in a short temperature range close to T_{sc} in superfluid ^3He under field, in the so-called A1 phase.¹⁵⁾ Theoretically, in the case of large spin-orbit coupling, a non-unitary state is expected in FM superconductors (due to band polarization), but it is excluded in orthorhombic paramagnetic superconductors left with only one dimensional representation¹⁶⁾ (they are possible only in the case of multiple second order transitions or of first order transition). However, the fact that H_{c2} in UTe_2 overcomes the Pauli limitation for all field directions supports the hypothesis that the d -vector can reorient under magnetic field, so that it should be considered in the weak spin-orbit coupling regime. Indeed, the alternative explanation for the absence of Pauli limitation along the hard axes, that the external field remains smaller than the internal exchange field¹⁷⁾ cannot apply in paramagnetic systems.

For such a weak spin-orbit coupling regime, multidimensional representations are allowed and non-unitary states are possible in paramagnetic materials.¹⁸⁾ These non-unitary states are extreme “equal spin pairing” (ESP) states, with only one of the two spin directions paired (d -vector of the form $\mathbf{d}(\mathbf{k}) = \varphi(\mathbf{k})(1, i, 0)$). So in UTe_2 , in contrast to the A1 phase of superfluid ^3He , this non-unitary state, where only half the FS is paired, would extend down to 0 K. The proposed mechanism for the stabilization of such an unfavorable state (half the condensation energy is lost) is through a linear coupling to the magnetization of the system,¹⁸⁾ strongly boosted here by the proximity to a FM instability. The SC transition would then give rise to a subdominant FM order parameter, reinforced by the transfer of spin-down electrons to spin-up state to gain condensation energy.¹⁹⁾

If this extreme non-unitary state is confirmed, it also means that the specific heat jump at T_{sc} is particularly large (more than twice the BCS value), as it should be compared to only half the normal state value. This definitely means that UTe_2 is in a strong coupling regime. This justifies the choice, in Ref. 11, of the strong coupling constant in zero field $\lambda \approx 0.75$ for the analysis of H_{c2} .

We also find that the entropy balance reveals that the normal state specific heat does not have a strictly constant γ -

value; the entropy at T_{sc} is $0.21 \text{ J K}^{-1} \text{ mol}^{-1}$ from the SC side, while the entropy at T_{sc} assuming a normal state with constant C_e/T is $0.19 \text{ J K}^{-1} \text{ mol}^{-1}$. The entropy discrepancy, approximately 10%, may imply a rapid increase of C_e/T in the normal state upon cooling due to the development of FM fluctuations. Note that, C/T at 0.39 K reaches $140 \text{ mJ K}^{-2} \text{ mol}^{-1}$ at a field close to H_{c2} for $H \parallel c$ -axis.¹³⁾ On the other hand, as shown in Fig. 2(a), the non-superconducting sample (#F) does not show any upturn of C_e/T down to 0.4 K. Its residual γ -value is about $\sim 140 \text{ mJ K}^{-2} \text{ mol}^{-1}$.

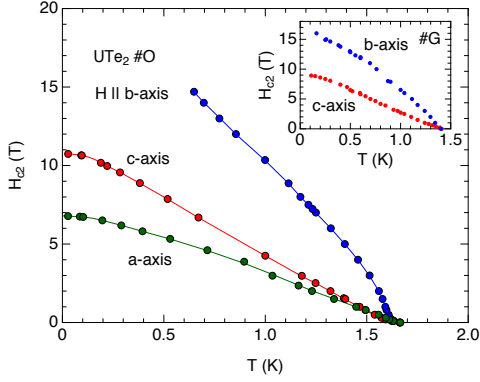


Fig. 3. (Color online) Temperature dependence of the superconducting upper critical field H_{c2} defined by the mid points of the resistivity drop for $H \parallel a$, b , and c -axes on sample #O in UTe_2 . The inset shows the H_{c2} curves for $H \parallel b$ and c -axes defined by zero resistivity on sample #G.

The temperature dependence of H_{c2} for $H \parallel a$, b , and c -axes in #O is shown in Fig. 3. Here the values of H_{c2} and T_{sc} are defined at the midpoint of the resistivity drop from the field/temperature scans. H_{c2} for $T \rightarrow 0 \text{ K}$ is extremely large. For $H \parallel a$ and c -axes, the values of $H_{c2}(0)$ are 6.8 and 10.7 T, respectively. For $H \parallel b$ -axis, $H_{c2}(0)$ highly exceeds our maximum field 15 T. The inset shows the H_{c2} curves defined by zero resistivity on a lower T_{sc} sample #G.

The Pauli limit of H_{c2} at 0 K for a singlet superconductor can be estimated as $H_P = \sqrt{2}\Delta/(g\mu_B) = 1.84T_{sc}$, assuming the free-electron value for the g -factor, $g = 2$, and a weak-coupling regime. Clearly, $H_{c2}(0)$ in UTe_2 violates this paramagnetic limit for all directions. With strong-coupling effects, the Pauli limit reaches higher values.¹⁴⁾ Using, for example, the value of the strong-coupling constant $\lambda = 0.75$ reported in Ref. 11, it would be possible to reproduce H_{c2} along the a -axis with $g < 0.5$. However, for $H \parallel c$ or b , and the same value of $\lambda = 0.75$, the violation of the Pauli limit is still too strong; the fitting H_{c2} with the Pauli limit for these directions would require a vanishing g -factor. Hence, indeed, the H_{c2} curves strongly support the absence of the Pauli limit and therefore spin triplet SC.

For $H \parallel a$ and c -axes, the temperature dependences of H_{c2} are similar to the previous results.¹¹⁾ However, the H_{c2} curve for $H \parallel b$ -axis is quite different from that in Ref. 11 at low temperature, where a strong increase of H_{c2} below 1.2 K is shown. On the other hand, we observe an anomalous linear increase up to 16 T at low temperature.

Figure 4 shows the angular dependence of H_{c2} from b to c -axis, and from b to a -axis. H_{c2} for $H \parallel b$ -axis at 30 mK

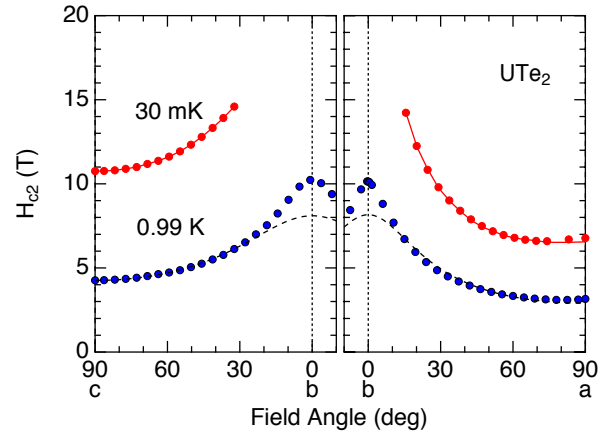


Fig. 4. (Color online) Angular dependence of H_{c2} at 30 mK and 0.99 K in UTe_2 for #O. The dotted lines at 0.99 K are the results of fitting by the effective mass model.

exceeds the maximum field, 15 T. H_{c2} decreases by tilting the field direction from b -axis. The decrease of H_{c2} from b to a -axis is more significant than that from b to c -axis, as expected from the anisotropy of H_{c2} . At 0.99 K, H_{c2} for $H \parallel b$ -axis is 10.2 T, revealing the maximum. The values of H_{c2} for $H \parallel b$ -axis determined from b to a -axis and from b to c -axis are almost identical, indicating that the misorientation for $H \parallel b$ -axis is negligibly small. The acute increase of H_{c2} near b -axis cannot be explained by the conventional effective mass model based on the assumption of an ellipsoidal FS, as shown in the dotted lines in Fig. 4.

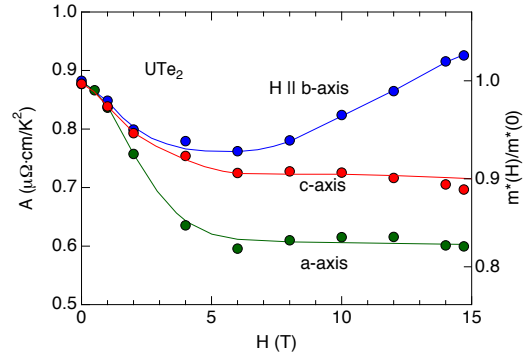


Fig. 5. (Color online) Field dependence of the resistivity A coefficient for $H \parallel a$, b , and c -axes in UTe_2 . The right axis shows the corresponding normalized effective mass, assuming the Kadowaki-Woods relation.

In order to capture the field dependence of the effective mass and its consequence on the strong coupling, the temperature dependence of the resistivity under magnetic field in the temperature range above T_{sc} was measured for $H \parallel a$, b , c -axes. The resistivity roughly follows the T^2 dependence up to $\sim 3.5 \text{ K}$ even at high fields. Thus we extract the resistivity A coefficients, as shown in Fig. 5. The results suggest the field dependence of the effective mass, as indicated in the right axis, based on the assumption of the Kadowaki-Woods relation, $A \propto \gamma^2 \propto m^{*2}$. The A coefficients decrease initially

for a , b , and c -axes, however above 5 T, a clear increase of A is detected only for $H \parallel b$ -axis. The broad maximum in the susceptibility for $H \parallel b$ -axis at $T_{\chi_{\max}} = 35$ K, which remains at least up to 5.5 T (not shown), suggests the metamagnetic-like transition at $H_m \sim 35$ T^{20,21} with an enhancement of the magnetic fluctuations associated with the FS change. It may set the large field-scale for an increase of $m^*(H)$ and thus $\lambda(H)$.

Let us comment on the differences observed in the three different results for $H \parallel b$ -axis between previous report¹¹ and our data (#O and #G). The most evident is the behavior of H_{c2} for $H \parallel b$, which displays a singular divergence only in Ref. 11. At first glance, one could believe that the new data presented here contradict this initial finding. However, closer inspection may reconcile all measurements. In Fig. 6(a), we show the experimental H_{c2} data together with the calculations of H_{c2} for different (constant) values of the strong coupling constant λ . These calculations are used to extract the field dependence $\lambda(H)$ required to reproduce the data. This is the same procedure as used for UCoGe and URhGe,²² and also for UTe₂,¹¹ all calculations are performed for a constant characteristic frequency (field independent) $\Omega = 34.3$ K, and a constant band Fermi velocity $v_{F,\text{band}} \approx 19200$ m/s. In the H_{c2} calculation, this band Fermi velocity is renormalized by $1/(1 + \lambda(H))$. The value of the band Fermi velocity was fixed to fit the H_{c2} for $H \parallel a$ of Ref. 11, (with a field independent $\lambda = 0.749$). Again, as for UCoGe and as done in Ref. 11, we assumed an isotropic Fermi velocity for all field directions, so that the much larger initial slope observed for $H \parallel b$ is explained by the strong initial increase of λ with field. The field dependence of λ for the three data sets are shown in Fig. 6(b).

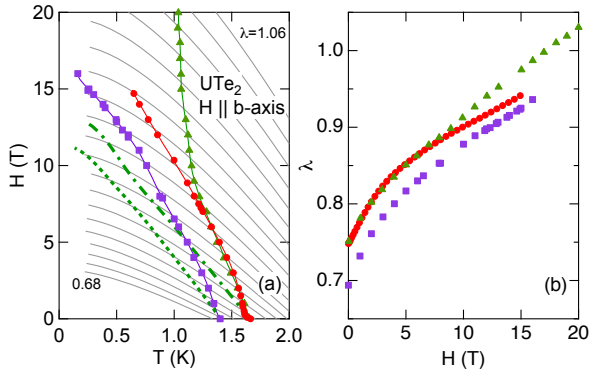


Fig. 6. (Color online) (a) Comparison of the three data set of H_{c2} for $H \parallel b$ in UTe₂ (green triangles,¹¹ red circles (#O), and violet squares (#G)). The gray solid lines are the H_{c2} calculations for λ varied between 0.68 and 1.06 by steps of 0.02, used to extract the values of $\lambda(H)$ to reproduce the different curves. The dashed dotted line is the calculated H_{c2} using the same $\lambda(H)$ which reproduces the diverging behavior,¹¹ but with an average initial Fermi velocity 15 % larger. The dashed line is the calculated H_{c2} using again the same $\lambda(H)$ in Ref. 11, but with 15 % smaller $T_{sc}(0)$ (characteristic frequency Ω is 15 % smaller). (b) Comparison of field dependence of λ required to reproduce the H_{c2} curves shown in panel (a), and with the same corresponding symbols. Note that although the behavior of H_{c2} shows no divergence in the present work, there are only minor differences between the different $\lambda(H)$.

First, let us note that although the temperature dependences of H_{c2} in the present work are quite different from the previous results,¹¹ the required field dependence of λ are very similar

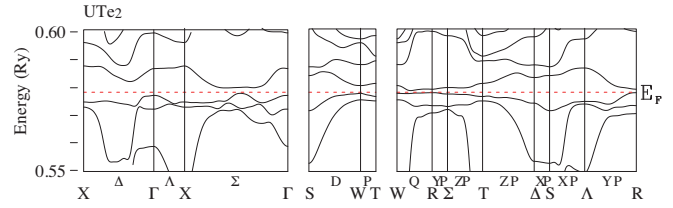


Fig. 7. (Color online) Band structure calculated by the LDA method near the Fermi energy in UTe₂. XP, YP, and ZP lines correspond to x , y , and z -planes with k_x , k_y , and $k_z = 0$, respectively.

for all data sets. In particular, $\lambda(H)$ for #G seems just shifted with respect to the previous one.¹¹ The same physics is at work in all samples. By contrast, the diverging behavior of H_{c2} is very sensitive to the exact balance between the orbital limitation of H_{c2} calculated at constant λ and the increase of $\lambda(H)$.

To illustrate this point, in Fig. 6(a), we show the calculated H_{c2} for the same $\lambda(H)$ reproducing the divergence in Ref. 11, but with a band Fermi velocity 15 % smaller, or with a T_{sc} 15 % smaller (obtained by reducing the characteristic frequency Ω by 15 %). In both cases, this is enough to completely suppress the divergence. The divergence requires that $\lambda(H)$ increases faster than the suppression of the superconducting state by the orbital limitation. UTe₂ seems to be very close to a perfect balance between both effects. As such, the system is certainly very sensitive to many parameters, for example, slight defects or impurities, or a slight change of stoichiometry (there is a solid solution of Te in U around the composition UTe₂). By shifting to the proximity to the FM instability or the change of the band structure, the behavior of H_{c2} might be drastically affected. Let us remark that the field window for the reentrant SC in URhGe shrinks as RRR decreases; the similar behavior is also observed for the field-reinforced SC in UCoGe.²⁾

A new perspective of UTe₂ is the Kondo semiconducting character which emerges in a LDA band structure calculations by using the structural parameters in Ref. 12. As shown in Fig. 7, there are very flat bands near the Fermi energy, E_F , which mainly consist of $5f$ electrons with $j = 5/2$. At E_F , a small energy gap (~ 130 K) is realized, indicating the semiconducting nature. The calculated results do not correspond to the real metallic electronic states at low temperature in UTe₂. Theoretically, to obtain correct sizes of FSs in f electron systems, it is sometimes required to shift the f level in self-consistent LDA calculations.²⁴ These results suggest that UTe₂ is most likely a semi-metal with heavy electronic states, which may have a very sensitive field-response.

In summary, we confirm SC by resistivity and specific heat experiments as well as a large residual γ -value below T_{sc} . The analysis of the resistivity suggests the increase of λ with field above 5 T for $H \parallel b$ -axis, in agreement with the behavior of H_{c2} . It should be clarified if the field response of λ in transverse field is dependent on the sample quality. Compared to the FM superconductors, UCoGe and URhGe, a main issue is to determine if UTe₂ remains paramagnetic below T_{sc} , or if SC is associated with its non-unitary order parameter to FM ordering. The divergence of H_{c2} for $H \parallel b$ -axis was not observed in our experiments. However, this may point out its

strong sensitivity to sample quality. The large residual γ -value below T_{sc} consistently found close to 50% of the normal phase value. This does support the very surprising proposal of a non-unitary state, where only half of the Fermi sea of a given spin direction would be paired. This can happen only if spin-orbit coupling is weak enough to avoid inducing SC on the opposite spin Fermi sheets. It also requires to induce a FM state on cooling below T_{sc} , which could be favored by the closeness to FM instabilities.

Acknowledgements

We thank Y. Tokunaga, S. Kambe, H. Sakai, S. Ikeda, Y. Ōnuki, K. Ishida, K. Izawa, V. Mineev, and S. Ran for fruitful discussion. This work was supported by ERC starting grant (NewHeavyFermion), KAKENHI (JP15H05884, JP15H05882, JP15K21732, JP16H04006, JP15H05745), and ICC-IMR.

- 1) D. Aoki and J. Flouquet: J. Phys. Soc. Jpn. **81**, 011003 (2012).
- 2) D. Aoki, K. Ishida, and J. Flouquet: J. Phys. Soc. Jpn. **88**, 022001 (2019).
- 3) S. S. Saxena, P. Agarwal, K. Ahilan, F. M. Grosche, R. K. W. Haselwimmer, M. J. Steiner, E. Pugh, I. R. Walker, S. R. Julian, P. Monthoux, G. G. Lonzarich, A. Huxley, I. Sheikin, D. Braithwaite, and J. Flouquet: Nature **406**, 587 (2000).
- 4) D. Aoki, A. Huxley, E. Ressouche, D. Braithwaite, J. Flouquet, J.-P. Brison, E. Lhotel, and C. Paulsen: Nature **413**, 613 (2001).
- 5) N. T. Huy, A. Gasparini, D. E. de Nijs, Y. Huang, J. C. P. Klaasse, T. Gortenmulder, A. de Visser, A. Hamann, T. Görlach, and H. v. Löhneysen: Phys. Rev. Lett. **99**, (2007) 067006.
- 6) F. Lévy, I. Sheikin, B. Grenier, and A. D. Huxley: Science **309**, 1343 (2005).
- 7) D. Aoki, T. D. Matsuda, V. Taufour, E. Hassinger, G. Knebel, and J. Flouquet: J. Phys. Soc. Jpn. **78**, 113709 (2009).
- 8) E. A. Yelland, J. M. Barraclough, W. Wang, K. V. Kamenev, and A. D. Huxley: Nature Phys. **7**, 890 (2011).
- 9) A. Gourgout, A. Pourret, G. Knebel, D. Aoki, G. Seyfarth, and J. Flouquet: Phys. Rev. Lett. **117**, 046401 (2016).
- 10) G. Bastien, A. Gourgout, D. Aoki, A. Pourret, I. Sheikin, G. Seyfarth, J. Flouquet, and G. Knebel: Phys. Rev. Lett. **117**, 206401 (2016).
- 11) S. Ran, C. Eckberg, Q.-P. Ding, Y. Furukawa, T. Metz, S. R. Saha, I.-L. Liu, M. Zic, H. Kim, J. Paglione, and N. P. Butch: arXiv:1811.11808.
- 12) S. Ikeda, H. Sakai, D. Aoki, Y. Homma, E. Yamamoto, A. Nakamura, Y. Shiokawa, Y. Haga, and Y. Ōnuki: J. Phys. Soc. Jpn. Suppl **75**, 116 (2006).
- 13) (Supplemental material) The field dependence of C/T is provided online.
- 14) L. N. Bulaevskii, O. V. Dolgov, and M. O. Pttisyn: Phys. Rev. B **38**, 11290 (1988).
- 15) A. J. Leggett: Rev. Mod. Phys. **47**, 331 (1975).
- 16) V. P. Mineev, K. V. Samokhin, *Introduction to unconventional superconductivity*, chapter 15, (Gordon and Breach Science Publishers, 1999)
- 17) V. P. Mineev: Phys. Rev. B **81**, 180504 (2010).
- 18) A.D. Hillier, J. Quintanilla, B. Mazidian, J.F. Annett, and R. Cywinski: Phys. Rev. Lett. **109**, 097001 (2012).
- 19) S. Takagi: Progress of Theoretical Physics **51** (1974) 1998.
- 20) D. Aoki, W. Knafo, and I. Sheikin: C. R. Physique **14**, 53 (2013).

- 21) W. Knafo, T. D. Matsuda, D. Aoki, F. Hardy, G. W. Scheerer, G. Ballon, M. Nardone, A. Zitouni, C. Meingast, and J. Flouquet: Phys. Rev. B **86**, 184416 (2012).
- 22) B. Wu, G. Bastien, M. Taupin, C. Paulsen, L. Howald, D. Aoki, and J.-P. Brison: Nature Commun. **8**, 14480 (2017).
- 23) V. P. Mineev, Physics-Uspekhi **60**, 121 (2017).
- 24) N. D. Dung, T. D. Matsuda, Y. Haga, S. Ikeda, E. Yamamoto, T. Ishikura, T. Endo, S. Tatsuoka, Y. Aoki, H. Sato, T. Takeuchi, R. Settai, H. Harima, and Y. Ōnuki: J. Phys. Soc. Jpn. **78**, 084711 (2009).
- 25) Y. Kasahara, T. Iwasawa, H. Shishido, T. Shibauchi, K. Behnia, Y. Haga, T. D. Matsuda, Y. Ōnuki, M. Sigrist, and Y. Matsuda: Phys. Rev. Lett. **99**, 116402 (2007).
- 26) S. Kittaka, Y. Shimizu, T. Sakakibara, Y. Haga, E. Yamamoto, Y. Ōnuki, Y. Tsutsumi, T. Nomoto, H. Ikeda, and K. Machida: J. Phys. Soc. Jpn. **85**, 033704 (2016).

Supplement

The field dependence of C/T in UTe_2 for $H \parallel c$ -axis in the SC state at 0.39 K and in the normal state at 1.8 K is shown in Fig. 8. In the SC state at 0.39 K, which corresponds to $0.25T_{sc}$, C/T increases rapidly with field and reaches $0.1 \text{ JK}^{-2}\text{mol}^{-1}$ at 0.4 T. It remains almost constant up to 1 T and then increases again with a moderate convex curvature. Further increasing field, C/T starts to decrease because of the collapse of the superconducting state at $H_{c2} \sim 8.6 \text{ T}$. Although the temperature is not low enough, the field dependence is not consistent with the isotropic superconducting gap, in which the linear increase of C/T is expected, implying the existence of the anisotropic gap with nodes. The steep increase at low field may suggest multiband SC, as is demonstrated in URu_2Si_2 .^{25,26)} In the normal state at 1.8 K, C/T is almost constant up to 9 T, in good agreement with the weak field dependence of the resistivity A coefficient, as shown in the main text.

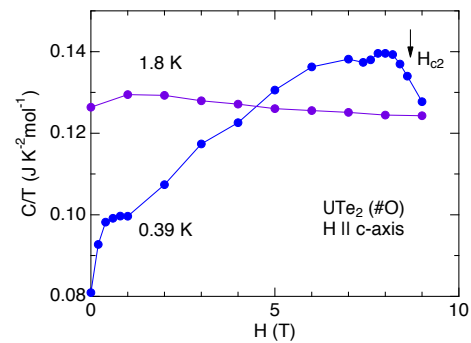


Fig. 8. (Color online) Field dependence of C/T at 0.39 K and 1.8 K for $H \parallel c$ -axis in UTe_2 for sample #O.